Experimental Constraint on an Exotic Parity-Odd Spin- and Velocity-Dependent Interaction with a Single Electron Spin Quantum Sensor

Man Jiao,[1,2,3] Maosen Guo,[1,2,3] Xing Rong,[1,2,3,*] Yi-Fu Cai,[4,5] and Jiangfeng Du[1,2,3,†]
[1]Hefei National Laboratory for Physical Sciences at the Microscale and Department of Modern Physics, University of Science and Technology of China, Hefei 230026, China
[2]CAS Key Laboratory of Microscale Magnetic Resonance, University of Science and Technology of China, Hefei 230026, China
[3]Synergetic Innovation Center of Quantum Information and Quantum Physics, University of Science and Technology of China, Hefei 230026, China
[4]CAS Key Laboratory for Research in Galaxies and Cosmology, Department of Astronomy, University of Science and Technology of China, Hefei 230026, China
[5]School of Astronomy and Space Science, University of Science and Technology of China, Hefei 230026, China

(Received 19 September 2020; accepted 2 June 2021; published 29 June 2021)

Improved laboratory limits on the exotic spin- and velocity-dependent interaction at the micrometer scale are established with a single electron spin quantum sensor. The single electron spin of a near-surface nitrogen-vacancy center in diamond is used as the quantum sensor, and a fused-silica half-sphere lens is taken as the source of the moving nucleons. The exotic interaction between the polarized electron and the moving nucleon source is explored by measuring the possible magnetic field sensed by the electron spin quantum sensor. Our experiment sets improved constraints on the exotic spin- and velocity-dependent interaction within the force range from 1.4 to 330 μm. The upper limit of the coupling $g_A^e g_V^N$ at 200 μm is $|g_A^e g_V^N| \leq 5.3 \times 10^{-19}$, significantly improving the current laboratory limit by more than 4 orders of magnitude.

DOI: 10.1103/PhysRevLett.127.010501

Experiments on searching for the interactions mediated by new particles beyond the standard model (SM) have achieved substantial development in the past decade [1,2]. Among various theoretical models beyond the SM, axions are a type of ultralight and *CP*-odd scalar fields that was originally put forward to address the issue of strong *CP* violation in the SM of particle physics via the Peccei-Quinn mechanism and later introduced as a candidate for dark matter particles [3–5]. Accompanied by novel strategies of detection technology, a wide observational window varying from astronomical instruments at cosmological scales to particle colliders at extremely microscopic scales has been explored (Chapter 111 in Ref. [6]). Recently, exotic spin-dependent interactions between fermions have been proposed that can be mediated by spin-1 bosons such as Z' bosons and paraphotons [7,8]. There are many ingenious experiments searching for exotic spin-dependent interaction among electrons and nucleons mediated by new bosons [9–14]. This type of laboratory experiment is sensitive to the particle physics properties of those hypothetical fields and hence provides a crucial approach to probing new physics beyond the SM [15].

In this work, we conducted a search for an exotic parity-odd spin- and velocity-dependent interaction between an electron spin and an unpolarized nucleon that is described by the potential [7]

$$V = g_A^e g_V^N \frac{\hbar}{4\pi} (\boldsymbol{\sigma} \cdot \boldsymbol{v}) \left(\frac{e^{-\frac{r}{\lambda}}}{r} \right), \tag{1}$$

where $\boldsymbol{\sigma}$ is the Pauli vector of the electron spin, g_A^e is the axial-vector coupling constant, and g_V^N is the nucleon vector coupling constant $r = |\boldsymbol{r}|$, with $\boldsymbol{r}$ being the displacement vector between the electron and nucleon, $\boldsymbol{v}$ the relative velocity, and $\lambda = \hbar/(m_b c)$ the force range, with m_b being the boson mass, c the speed of light in vacuum, and $\hbar$ the Planck's constant divided by 2π. The first parity-odd interaction via W exchange in the weak interaction sector was observed in the Wu experiment [16], but this interaction was negligible at the micrometer scale. The exotic parity-odd spin- and velocity-dependent interaction discussed in this Letter can be mediated by massive spin-1 bosons [8]. Experimental searches for exotic spin-dependent interactions could be important for understanding and developing theories beyond the SM. Such interaction leads to an effective magnetic field sensed by the electron spin arising from the moving nucleons:

$$\boldsymbol{B}(r) = \frac{g_A^e g_V^N}{2\pi\gamma_e} \boldsymbol{v} \frac{e^{-r/\lambda}}{r}, \tag{2}$$

where γ_e is the gyromagnetic ratio of the electron spin. Recently, experimental upper bounds on this interaction have

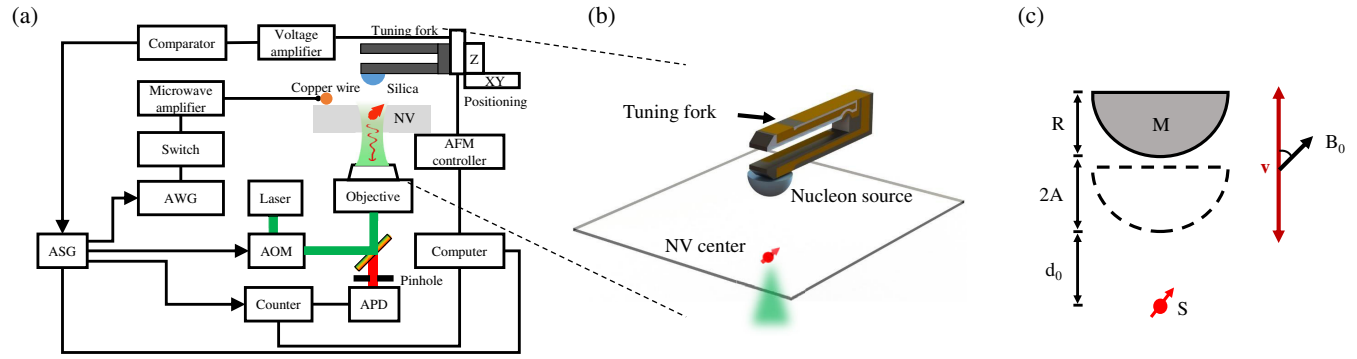

FIG. 1. (a) Schematic diagram of the experimental setup. The 532 nm pulsed laser passed twice through an acousto-optic modulator (AOM) and an objective before being focused on the NV center. The red fluorescence was collected by an avalanche photodiode (APD) with a counter. The microwave pulses were generated by a 12 GSa/s arbitrary waveform generator (AWG), amplified by a microwave power amplifier, and then delivered via a copper wire. An arbitrary sequence generator (ASG) [26] has been used to synchronize the whole setup. Atomic force microscopy (AFM) has been installed to drive and monitor the vibration of the tuning fork. (b) The detailed figure for the single NV center and the tuning fork. A fused-silica half-sphere, labeled as "Nucleon source," is used as a moving mass source. (c) A schematic diagram of interacting source and the single electron spin sensor. The radius of the nucleon source, M, is $R = 250$ μm. A static magnetic field $\boldsymbol{B}_0$ was applied along the symmetry axis of the NV center (S). $\boldsymbol{v}$ is the relative velocity vector between the NV center and the half-sphere lens. θ stands for the angle between the velocity vector and the external magnetic field $\boldsymbol{B}_0$.

been set by laboratory experiments such as the atomic parity nonconservation [17], spin-exchange-relaxation-free atomic magnetometer [18], and electron-spin polarized torsion pendulum [19] experiments.

We used a single electron spin of a near-surface nitrogen-vacancy (NV) center in diamond as a detector for testing the exotic parity-odd interaction. Single NV centers in diamond are defects composed of a substitutional nitrogen atom and a neighboring vacancy [20]. They have been applied as nanoscale quantum sensors for detecting weak magnetic fields [21,22]. Recently, NV centers have been demonstrated as detectors for exploring the electron-nucleon monopole-dipole interaction [12] and axial-vector mediated interaction between polarized electrons [13]. Because of the size of the sensor, which can be engineered to be small compared to the micrometer force range, the geometry of the sensor enables close proximity between the sensor and the source. Furthermore, delicate quantum control methods, such as dynamical decoupling techniques [23], can be employed to suppress the unwanted magnetic noise to enhance the sensitivity of the sensor [24].

Our experiment was carried out on a magnetometer based on a single NV center as shown in Fig. 1. A similar setup was used for testing the static monopole-dipole interaction mediated by pseudo-scalar bosons between an electron spin and nucleons [12]. Figures 1(a) and (b) show the schematic of our experimental setup. The single NV center is close to the surface of the diamond with a depth of less than 10 nm. This NV center was created by implantation of 10 keV N_2^+ ions into a $\langle 100 \rangle$ bulk diamond and annealing for two hours at 800 °C. After annealing, the diamond was oxidatively etched for 4 hours at 580 °C. We fabricated nanopillars on the surface of the diamond to enhance the detection efficiency of the photoluminescence. The average photoluminescence rate in this experiment has achieved to be 350 kcounts/s with a laser power of about 200 μW. The ground state of the NV center is an electron spin triplet state $^3A_2$ with three substates $|m_S = 0\rangle$ and $|m_S = \pm 1\rangle$. We applied an external magnetic field along the symmetry axis of the NV center to remove the degeneracy of the $|m_S = \pm 1\rangle$ spin states. The strength of the magnetic field was set to be 565Gauss, and green laser pulses can initialize the state of NV center to be $|m_S = 0\rangle$. The microwave pulses used to manipulate the quantum states of the NV center are delivered by a copper wire placed on the surface of the diamond. We encode two spin states, $|m_S = 0\rangle$ and $|m_S = -1\rangle$, as a quantum sensor that is sensitive to the magnetic field. The dephasing time of the electron spin obtained from the spin echo [25] experiment is 27(4) μs. The source of the mass is a fused-silica half-sphere lens with a diameter of 500 μm. The lens is installed on one prong of the tuning fork. This is a movable mass source, which enables the detection of the exotic spin- and velocity-dependent interactions. Hereafter, the single electron spin of NV center and the moving mass source are denoted as S and M for convenience, respectively.

The geometric parameters of the setup are presented in Fig. 1(c). Since M is driven by the tuning fork, the distance between S and the bottom of M is $d(t) = d_0 + A[1 + \cos(\omega_M t)]$, where d_0 is the minimal distance and A and ω_M are the amplitude and angular frequency of M, respectively. The velocity of M is $v(t) = -A\omega_M \sin(\omega_M t)$. An external magnetic field $\boldsymbol{B}_0$ is applied along the NV axis. The angle between the direction of the velocity $\boldsymbol{v}$ and the magnetic field $\boldsymbol{B}_0$ is $\theta = \arccos(1/\sqrt{3})$. The effective magnetic field on S along the NV axis arising from the hypothetic spin- and velocity-dependent interaction can be

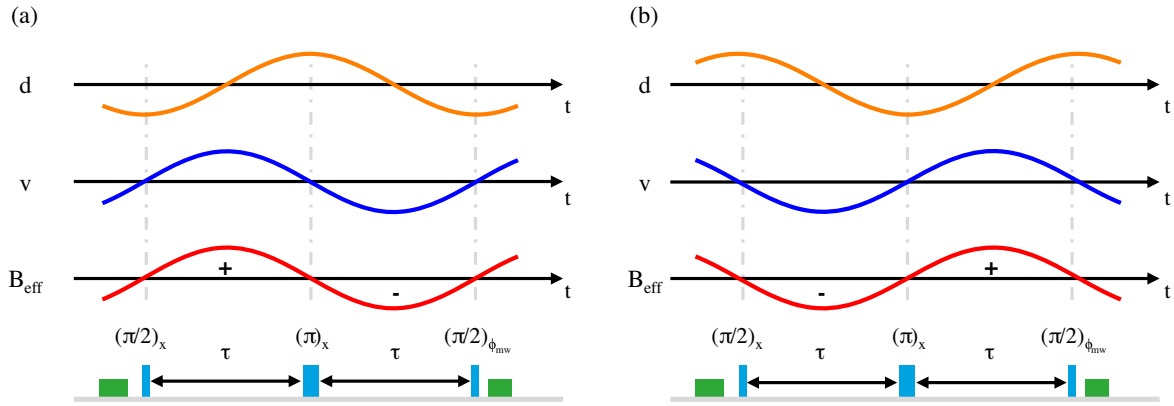

FIG. 2. Experimental scheme of testing the parity-odd spin- and velocity-dependent interaction between a single spin and a moving mass source. (a) and (b) are, respectively, experimental pulse sequences for accumulating a positive and negative phase factor due to the exotic interaction on the superposition state of S. Symbols π and $\pi/2$ stand for the rotation angles of the quantum state due to the microwave pulses. The phase of the last $\pi/2$ microwave pulse is ϕ_{mw}. For accumulating a positive (negative) phase factor, the $\pi/2$ microwave pulses were applied on S when M passed through the minimal (maximum) value of d(t). π microwave pulses were applied on the center of the microwave sequence. The time duration between $\pi/2$ and π pulses is $\tau = \pi/\omega_M$. The pulse lengths of $\pi/2$ and π are 64 ns and 127 ns, respectively. The time durations of the green laser pulse for initialization and readout are 2.0 μs and 0.3 μs, respectively. The waiting time τ is 6.652 μs.

derived from integrating $\boldsymbol{B}(r)$ over all nucleons in the half-sphere lens as

$$\boldsymbol{B}_{\mathrm{eff}} = \frac{g_A^e g_V^N}{2\pi\gamma_e} f(\lambda, R, d)\boldsymbol{v}\cos\theta, \tag{3}$$

where $f(\lambda, R, d) = 2\pi\rho\lambda^2\{-e^{-(d+R)/\lambda} + e^{-d/\lambda} + \{[\sqrt{R^2 + (d+R)^2} + \lambda]/(d+R)\}e^{-(\sqrt{R^2+(d+R)^2})/\lambda} - [(d+\lambda)/(d+R)]e^{-d/\lambda}\}$ and $\rho = 1.33 \times 10^{30}$ m^{-3} is the number density of nucleons in M. Since the tuning fork is made of silica, the contribution of the tuning fork is also taken into account (see the Supplemental Material for details [27]).

Figure 2 shows the experimental pulse sequence for exploring the exotic interaction. In Fig. 2(a), we show how to accumulate a phase factor due to the possible interaction on the superposition state of S. The time evolution of distance d(t) (orange line), the velocity of M, v(t) (blue line), and the possible B_{eff}(t) (red line) due to the moving nucleons are presented (top three illustrations), along with the laser and the microwave pulse sequences that were applied on S for initializing, manipulating, and reading out the states of the single spin S (bottom illustration). The laser and microwave pulse sequences were synchronized with the vibration of M with a pulse generator and a comparator [12,26]. The first laser pulse and the following $\pi/2$ microwave pulse were used to convert the state of S to a superposition state $(|0\rangle - i|-1\rangle)/\sqrt{2}$. The $\pi/2$ microwave pulses were applied on S when M passed through the minimal values of d(t). In this case, during the first waiting time τ, the state of spin evolves about the z axis and accumulates a positive phase factor dependent on the magnetic field $\boldsymbol{B}_{\mathrm{eff}}$, while S will accumulate a negative phase factor during the second waiting time. Because of the π pulse inverting the state of S in the middle of the time evolution, the final state of S acquires a positive phase factor. After the last $\pi/2$ pulse with a variable phase ϕ_{mw}, the population of the final state on $|m_S = 0\rangle$ can be written as $P_+ = [1 + \cos(\phi_{\mathrm{mw}} + \phi)]/2$ with $\phi = \int_0^\tau \gamma_e \boldsymbol{B}_{\mathrm{eff}}(t)dt - \int_\tau^{2\tau} \gamma_e \boldsymbol{B}_{\mathrm{eff}}(t)dt$. In Fig. 2(b), the final state is designed to acquire a negative phase factor with $\pi/2$ pulses being applied on S when M passed through the maximum values of d(t). The population of the final state on $|m_S = 0\rangle$ in this case can be written as $P_- = [1 + \cos(\phi_{\mathrm{mw}} - \phi)]/2$. In our experiment, we recorded the difference between the two populations,

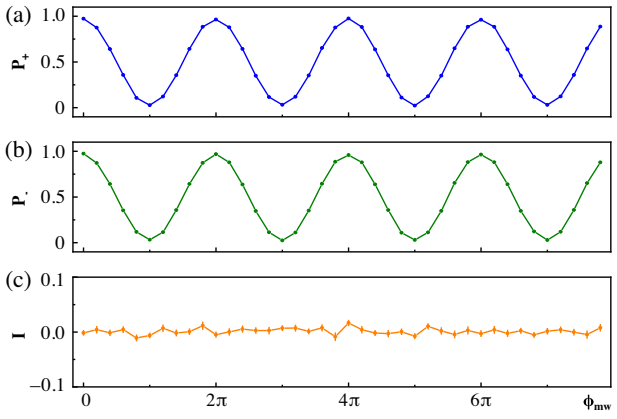

FIG. 3. Experimental results for testing the parity-odd spin- and velocity-dependent interaction. (a) and (b) are experimental data for population of the final state on $|m_S = 0\rangle$, P_+, and P_-, respectively. (c) Orange dots with error bars are the difference between P_+ and P_-.

TABLE I. Summary of the systematic errors in our experiments. The corrections to the constraint on $g_A^e g_V^N$ with $\lambda = 200$ μm are listed.

Parameter	Value	$\Delta g_A^e g_V^N (\times 10^{-19})$
θ	$54.7 \pm 0.6°$	$^{+0.075}_{-0.078}$
Distance between M and S	2.0 ± 0.1 μm	± 0.004
Diameter of M	500 ± 2.5 μm	± 0.014
Thickness of M	250 ± 35 μm	$^{+0.002}_{-0.005}$
Amplitude of vibration	165.2 ± 0.1 nm	± 0.003
Deviation in x-y plane	1.3 ± 0.8 μm	± 0.001
Final $g_A^e g_V^N (\times 10^{-19})$	1.48	± 1.84 (statistic)
		± 0.08 (systematic)

$I = P_+ - P_- = -\sin(\phi_{\rm mw})\sin(\phi)$. A detailed data analysis has been included in the Supplemental Material [27].

In our experiment, the time duration is $\tau = 6.652$ μs, the amplitude of the vibrating M is $A = 165.2(1)$ nm, and the angular frequency $\omega_M = 2\pi \times 74.45$ kHz. The minimal distance between the NV center and the bottom of the half-sphere is $d_0 = 2.0(1)$ μm. We repeated the measurement 6×10^7 times to build good statistics. Figure 3 shows the experimental results. These results show that the parameter $\phi = 0.0011 \pm 0.0014$ rad can be obtained by fitting the data with $I = -\sin(\phi_{\rm mw})\sin(\phi)$. For the force range $\lambda = 200$ μm, the coupling is estimated to be $(1.48 \pm 1.84) \times 10^{-19}$, and there is no exotic parity-odd spin- and velocity-dependent interaction observed in the current experiment. Nevertheless, an experimental limit on such interaction can be obtained from our experiment.

Table I provides the systematic error budget of our experiment, where we take $\lambda = 200$ μm as an example. The systematic errors are mainly due to the uncertainties of several parameters of the setup, such as the angle between $\boldsymbol{B}_{\rm eff}$ and the NV axis, the minimal distance between M and S, and the amplitude of the vibration of M. The uncertainty of the diameter and the thickness of the half-sphere lens have also been taken into account. In the Supplemental Material [27], we show that the effect of the modulated magnetic field due to the diamagnetism of M and the tuning fork can be canceled by our experimental sequence [27]. Experimental measurements show that there was no observable signal from the tuning fork [27]. Since the NV center did not locate exactly under the center of the half-sphere, the misalignment between the NV center and the half-sphere in the x-y plane is considered as a source of systematic error. Combining these systematic errors in quadrature, the total systematic error is derived to be $\pm 0.08 \times 10^{-19}$. The bound from our experiment for the interaction with the force range being 200 μm is $|g_A^e g_V^N| \leq 5.3 \times 10^{-19}$ with a 95% confidence level when both statistical and systematic errors are taken into account. The other values of upper bound with different values of force range can be obtained with the same method.

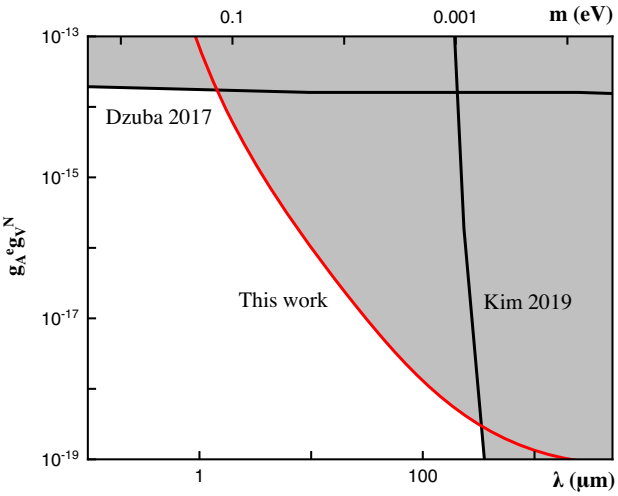

FIG. 4. Upper limit on the exotic parity-odd spin- and velocity-dependent interaction $g_A^e g_V^N$ as a function of the force range λ and mass of the bosons m_b. Black lines are upper limits established by experiments in Refs. [17,18]. The red line is the upper bound obtained from our experiment, which establishes an improved laboratory bound in the force range from 1.4 to 330 μm. The upper limit of the coupling $g_A^e g_V^N$ at 200 μm is $|g_A^e g_V^N| \leq 5.3 \times 10^{-19}$, which is significantly improved by up to 4 orders of magnitude.

Figure 4 shows the upper bounds on the parity-odd spin- and velocity-dependent interaction between the polarized electron and unpolarized nucleon established by this work, together with recent constraints. The gray filled areas are excluded from experimental searches. For force range $\lambda > 330$ μm, the strongest constraints were set by Kim *et al.* when an optically polarized vapor magnetometer with Rb electron spin and BGO nucleon source was used to search for this interaction [18]. For the force range $\lambda < 1.4$ μm, the upper bounds were established from atomic parity nonconservation experiments by Dzuba *et al.* [17]. For the force range from 1.4 to 330 μm, the best experimental bounds are obtained from our experiment as the red line shown in Fig. 4. The experimental upper limit for the force range $\lambda = 200$ μm is $|g_A^e g_V^N| \leq 5.3 \times 10^{-19}$, which is more than 4 orders of magnitude more stringent than the bound established in the previous result in Ref. [17].

In summary, we report an experimental search for a type of parity-odd spin- and velocity-dependent interaction. A single electron spin of an NV center in diamond has been used as a quantum sensor for detecting the possible magnetic field due to the exotic interaction between the electron spin and a moving mass source. The current experimental sensitivity is mainly limited by the coherence time of the NV center quantum sensor, which can be further improved by using a deeper NV center. The ensemble NV centers system, which provides better magnetic field sensitivity [34,35], can also be used to search for exotic

spin-dependent interactions in future. In addition, our experimental setup has been modified to search for the exotic parity-even spin- and velocity-dependent interactions between polarized electrons and nucleons where the direction of the velocity of the mass source has been set parallel to the surface of the diamond [36]. Our result shows that an NV-based quantum sensing setup can be used as a promising platform, not only for physics within the standard model but also for searching interactions predicted by physics beyond the standard model.

The authors are grateful to the anonymous referees for their valuable comments. This work was supported by the National Key R&D Program of China (Grants No. 2018YFA0306600 and No. 2016YFB0501603), the National Natural Science Foundation of China (Grants No. 11722327, No. 11961131007, and No. 11653002), the Chinese Academy of Sciences (Grants No. GJJSTD20170001, No. QYZDY-SSW-SLH004, and No. QYZDB-SSW-SLH005), and the Anhui Initiative in Quantum Information Technologies (Grant No. AHY050000). X. R. thanks the Youth Innovation Promotion Association of Chinese Academy of Sciences for its support. Y. F. C. is supported in part by the CAST Young Elite Scientists Sponsorship Program (2016QNRC001) and by the Fundamental Research Funds for the Central Universities.

M. J. and M. G. contributed equally to this work.

*Corresponding author.
xrong@ustc.edu.cn
†Corresponding author.
djf@ustc.edu.cn

[1] J. E. Moody and F. Wilczek, Phys. Rev. D **30**, 130 (1984).
[2] M. S. Safronova, D. Budker, D. DeMille, D. F. J. Kimball, A. Derevianko, and C. W. Clark, Rev. Mod. Phys. **90**, 025008 (2018).
[3] R. D. Peccei and H. R. Quinn, Phys. Rev. Lett. **38**, 1440 (1977).
[4] S.Weinberg, Phys. Rev. Lett. **40**, 223 (1978).
[5] J. E. Kim and G. Carosi, Rev. Mod. Phys. **82**, 557 (2010).
[6] M. Tanabashi *et al.* (Particle Data Group Collaboration), Phys. Rev. D **98**, 030001 (2018).
[7] B. A. Dobrescu and I. Mocioiu, J. High Energy Phys. 11 (2006) 005.
[8] P. Fadeev, Y. Stadnik, F. Ficek, M. G. Kozlov, V. V. Flambaum, and D. Budker, Phys. Rev. A **99**, 022113 (2019).
[9] N. Crescini, C. Braggioa, G. Carugnoa, P. Falferib, A. Ortolanc, and G. Ruoso, Nucl. Instrum. Methods Phys. Res., Sect. A **842**, 109 (2017).
[10] J. Lee and M. Romails, Phys. Rev. Lett. **120**, 161801 (2018).
[11] Y. V. Stadnik, V. A. Dzuba, and V. V. Flambaum, Phys. Rev. Lett. **120**, 013202 (2018).
[12] X. Rong *et al.*, Nat. Commun. **9**, 739 (2018).
[13] X. Rong, M. Jiao, J. Geng, B. Zhang, T. Xie, F. Shi, C.-K. Duan, Y.-F. Cai, and J. Du, Phys. Rev. Lett. **121**, 080402 (2018).
[14] M. Jiao, X. Rong, H. Liang, Y. Cai, and J. Du, Phys. Rev. D **101**, 115011 (2020).
[15] D. DeMille, J. M. Doyle, and A. O. Sushkov, Science **357**, 990 (2017).
[16] C. S. Wu, E. Ambler, R. W. Hayward, D. D. Hoppes, and R. P. Hudson, Phys. Rev. **105**, 1413 (1957).
[17] V. A. Dzuba, V. V. Flambaum, and Y. V. Stadnik, Phys. Rev. Lett. **119**, 223201 (2017).
[18] Y. Kim, P. Chu, I. Savukov, and S. Newman, Nat. Commun. **10**, 2245 (2019).
[19] B. R. Heckel, E. G. Adelberger, and C. E. Cramer, Phys. Rev. D **78**, 092006 (2008).
[20] A. Gruber, A. Drbenstedt, C. Tietz, L. Fleury, J. Wrachtrup, and C. von Borczyskowski, Science **276**, 2012 (1997).
[21] R. Schirhagl, K. Chang, M. Loretz, and C. L. Degen, Annu. Rev. Phys. Chem. **65**, 83 (2014).
[22] C. L. Degen, F. Reinhard, and P. Cappellaro, Rev. Mod. Phys. **89**, 035002 (2017).
[23] J. Du, X. Rong, N. Zhao, Y. Wang, J. Yang, and R. B. Liu, Nature (London) **461**, 1265 (2009).
[24] J. M. Taylor, P. Cappellaro, L. Childress, L. Jiang, D. Budker, P. R. Hemmer, A. Yacoby, R. Walsworth, and M. D. Lukin, Nat. Phys. **4**, 810 (2008).
[25] E. Hahn, Phys. Rev. **80**, 580 (1950).
[26] X. Qin, Y. J. Xie, R. Li, X. Rong, X. Kong, F. Z. Shi, P. F. Wang, and J. F. Du, IEEE Magn. Lett. **7**, 1 (2016).
[27] See Supplemental Material, which includes Refs. [28–33], at http://link.aps.org/supplemental/10.1103/PhysRevLett.127.010501 for details of the experimental setup and statistical and systematic error analysis.
[28] J. Liu, A. Callegari, M. Stark, and M. Chergui, Ultramicroscopy **109**, 81 (2008).
[29] O. E. Dagdeviren, Y. Miyahara, A. Mascaro, and P. Grütter, Rev. Sci. Instrum. **90**, 013703 (2019).
[30] J. F. Ziegler, M. D. Ziegler, and J. P. Biersack, Nucl. Instrum. Methods Phys. Res., Sect. B **268**, 1818 (2010).
[31] J. Wang, W. Zhang, J. Zhang, J. You, Y. Li, G. Guo, F. Feng, X. Song, L. Lou, W. Zhu, and G. Wang, Nanoscale **8**, 5780 (2016).
[32] V. Jacques, P. Neumann, J. Beck, M. Markham, D. Twitchen, J. Meijer, F. Kaiser, G. Balasubramanian, F. Jelezko, and J. Wrachtrup, Phys. Rev. Lett. **102**, 057403 (2009).
[33] L. Childress, M. V. Gurudev Dutt, J. M. Taylor, A. S. Zibrov, F. Jelezko, J. Wrachtrup, P. R. Hemmer, and M. D. Lukin, Science **314**, 281 (2006).
[34] Y. Xie, H. Yu, Y. Zhu, X. Qin, X. Rong, C.-K. Duan, and J. Du, Sci. Bull. **66**, 127 (2021).
[35] J. F. Barry, J. M. Schloss, E. Bauch, M. J. Turner, C. A. Hart, L. M. Pham, and R. L. Walsworth, Rev. Mod. Phys. **92**, 015004 (2020).
[36] X. Rong, M. Jiao, M. S. Guo, D. G. Wu, and J. F. Du, arXiv:2010.15667.